BMC Cancer

RESEARCH Open Access

In situ phenotypic and karyotypic co-detection of aneuploid TCs and TECs in cytological specimens with abnormal cervical screening results

Yanling Wang[1], Alexander Y. Lin[2], Daisy Dandan Wang[2], Peter Ping Lin[2], Xuexin Zhou[1], Yongbin Yang[1*] and Yaping Zhu[1*]

Abstract

Background To distinguish and co-detect aneuploid CD31$^-$ tumor cells (TCs) and CD31$^+$ tumor endothelial cells (TECs) may have significant diagnostic values for cervical cancer screening. However, there are very few relevant studies. In the present study, a novel "immunofluorescence staining integrated with fluorescence in situ hybridization (iFISH)" tumor tissue biopsy platform was applied to comprehensively investigate the clinical utilities of aneuploid TCs and TECs in all-stage cervical lesion smear specimens.

Methods A total of 196 patients were enrolled in this study. Immunofluorescence staining of p16 and Ki67 combined with FISH was applied to quantitatively co-detect and characterize subcategorized aneuploid CD31$^-$ TCs and CD31$^+$ TECs in cervical cytological specimens. The Kruskal–Wallis H test was used to compare the distributions of aneuploid TCs and TECs among all stages of cervical lesions and among the different high-risk HPV types (HPV16/18 and non-HPV16/18). The diagnostic value of detecting aneuploid TCs and TECs for high-grade squamous intraepithelial lesions (HSIL$^+$) was investigated via receiver operating characteristic curve analysis.

Results The number of total aneuploid CD31$^-$ TCs and their p16$^+$ and/or Ki67$^+$ (p16/Ki67$^+$) subtypes increased markedly with the severity of cervical lesions, although a similar trend was not observed for aneuploid CD31$^+$ TECs. The increase in aneuploid TCs resulted from HPV16/18 infection was mainly concentrated in low-grade squamous intraepithelial lesion(LSIL), whereas the increase caused by non-HPV16/18 infection was mainly concentrated in HSIL. To identify HSIL$^+$, the area under the curve (AUC) of tetraploid TCs was the largest (0.739), followed by multiploid (≥ pentaploid) TCs (0.724) and triploid TCs (0.699). For the combined subtypes, the AUC of ≥ tetraploid TCs was 0.745, and their unique diagnostic value was clinically reflected by their high specificity.

Conclusion The quantity of CD31$^-$ aneuploid TCs was associated with the severity of cervical lesions. In HPV16/18 positive patients, aneuploid CD31$^-$ TCs were significantly increased in the LSIL. Moreover, aneuploid CD31$^-$ TCs exhibited remarkable specificity for detecting HSIL$^+$. Further studies are required to expand the potential clinical utility of detecting CD31$^-$ aneuploid TCs.

*Correspondence:
Yongbin Yang
yybvsywz@163.com
Yaping Zhu
zhuyp63@126.com
Full list of author information is available at the end of the article

Keywords Cervical cancer, Aneuploid TCs and TECs, iFISH tumor tissue biopsy, Chromosome 8, p16 and Ki67, HPV16/18

Background

Cervical cancer is the fourth most common malignant tumor in women and severely threatens female health. According to Global Cancer Statistics 2020, more than 600,000 new cases and more than 340,000 mortality are estimated yearly [1]. Carcinogenic human papillomavirus (HPV) infection is the most critical condition for cervical cancer. However, HPV infection has a long-term natural history before it progresses to cervical cancer. Additionally, premalignant lesions known as cervical intraepithelial neoplasia (CIN) have varied in severity over several years or more than a decade [2], providing an excellent "window" for the prevention and treatment of cervical cancer. HPV vaccination and cervical screening are the most effective ways to prevent cervical cancer. Given the low rates of vaccination in China [3], cervical screening remains the first line of prevention for cervical cancer. High-risk HPV (hrHPV) testing is the primary screening method with high sensitivity. Many patients have "transient" infections, necessitating the triage of women with hrHPV infection. Although it is the most frequently used triage strategy, cytological testing has inherent limitations that rely on the training and experience of the pathologist, is strongly subjective, and lacks quality control, which inevitably increases the rate of misdiagnosis [4–6]. Several studies have focused on new biomarkers and cervical screening techniques to maximize the cost-efficiency of patients.

Aneuploidy refers to the gain or loss of chromosomes, a common characteristic of malignant tumors, and occurs in 90% of solid tumors [7]. It is an early event of tumorigenesis and can participate in tumor formation and development, such as affecting the cell cycle and genomic stability, producing a protein stress response, interfering with cell metabolism, and altering the tumor microenvironment [7–9]. A high frequency of aneuploidy is associated with invasion, metastasis, and poor prognosis in various types of tumors. Previous studies have shown that hrHPV infection is related to the development of aneuploidy and positively correlated with the severity of cervical lesions [10, 11]. Thus, designing a strategy capable of detecting aneuploidy in these abnormal cells may have clinical value in the early diagnosis of cervical lesions, especially high-grade lesions.

Immunofluorescence staining integrated with fluorescence in situ hybridization (iFISH) is a new detection technique combining protein immunofluorescence staining and chromosome karyotype detection to identify and characterize subclasses of aneuploid TCs and TECs [12]. Some previous studies performed by others applied FISH alone to analyze chromosomal copy number aberrations in exfoliated cervical cells. Preliminary results showed that the frequency of chromosomal aberrations in exfoliated cervical cells varies with the stage of the cervical lesion [10, 13, 14]. Furthermore, these chromosomal aberrations also vary based on different HPV genotypes [15], which may guide personalized management of precancerous lesions. Previous studies have focused mainly on changes in some chromosome sites, and limited data on the chromosomal karyotype have been collected. In addition, these studies were incapable of combining tumor marker staining simultaneously. Therefore, there is insufficient evidence on the use of chromosomal karyotype changes with tumor marker staining in the clinical diagnosis of cervical lesions, and several studies are needed to quantify the risk stratification of cervical lesions.

In the present study, we used iFISH tumor tissue biopsy technology to detect aneuploidy in exfoliated cervical cells from patients referred for colposcopy and selected centromere probe 8 (CEP8) to estimate chromosome ploidy and p16 and Ki67 as tumor markers [16]. In addition, an anti-CD31 immunostaining was applied to distinguish TECs which also exhibit aneuploidy and participate in tumor progression and metastasis [17, 18]. Different subtypes of aneuploid TCs and TECs were subsequently screened on the basis of the above characteristics. Next, we assessed the differences in chromosome ploidy and explored the diagnostic accuracy of various subclasses of aneuploid TCs and TECs for detecting high-grade cervical lesions.

Materials and methods

Patients and samples

A total of 196 subjects (clinical characteristics were presented in Table 1) treated at the North Campus of Shanghai General Hospital (Shanghai, China) between August 2022 and March 2023 were enrolled in this study. All subjects were referred for colposcopy due to either HPV positivity or abnormal cytological results (according to the American Society for Colposcopy and Cervical Pathology (ASCCP) guidelines [19]). Prior to colposcopy, cytology samples were collected from the cervical canal and the transformation zone with a cell brush and transferred to Cell Preservation Solution (Cytelligen, San Diego, CA, USA). The

Table 1 Clinical characteristics of 196 enrolled individuals

		N(percentage,%)
Age(mean,range)		43 (21–78)
The stage of cervical lesion		
Normal		70(35.7%)
LSIL		53(27.0%)
HSIL		51(26.0%)
Cancer		22(11.2%)
	HPV type	
Normal	HPV16/18	41(20.9%)
	non-HPV16/18	29(14.8%)
LSIL	HPV16/18	23(11.7%)
	non-HPV16/18	30(15.3%)
HSIL	HPV16/18	22(11.2%)
	non-HPV16/18	29(14.8%)
Cancer	HPV16/18	17(8.7%)
	non-HPV16/18	5(2.6%)

exclusion criteria in this study were as follows: (A) acute inflammatory period (acute cervicitis), sexual life within 24 h; (B) menstruation, pregnancy, or postpartum within 42 days; (C) history of total hysterectomy, cervical surgery, or cervical physical therapy within 3 months; and (D) receiving pelvic radiation therapy at any time previously or having a history of other malignancies.

Colposcopy and pathological results

Macroscopic cervical lesions were directly biopsied via colposcopy conducted by skilled gynecologists. If these lesions were invisible, biopsies were randomly taken from 3, 6, 9, and 12 points of the cervix. All high-grade squamous intraepithelial lesion (HSIL) patients were hospitalized for standardized treatment. The histopathological results of both colposcopy biopsies and surgical samples were considered, and the highest pathological index of the cervix was the final diagnosis. All the samples were processed via standard histopathological procedures, and two pathologists evaluated the results in a double-blinded manner. The final diagnosis was confirmed by the chief pathologist. The pathological examination results were classified as normal (including cervicitis), low-grade squamous intraepithelial lesion (LSIL, equal to CIN1), HSIL (equal to CIN2-3), and cervical cancer. The final diagnoses of the subjects included in this study were as follows: 70 patients with normal cervix, 53 patients with LSIL, 51 patients with HSIL, and 22 patients with cervical cancer.

iFISH tumor tissue biopsy of cervical scraping smear samples

iFISH tumor tissue biopsy was applied to detect aneuploid $CD31^-$ TCs and $CD31^+$ TECs expressing tumor markers in cervical smear specimens stored in Cell Preservation Solution (Cytelligen). The samples were processed according to the manufacturer's protocol (Cytelligen). Briefly, samples without floccules were clarified by centrifugation at 500 × g at room temperature for 5 min, followed by transferring the sedimented cells into a 1.5-mL Eppendorf tube containing 800 mL of Circulating Rare Cell (CRC) buffer. The samples were thoroughly homogenized via a syringe. The pellet was obtained by centrifugation at 2300 × g for 3 min and resuspended in 100 mL of CRC buffer plus 2 mL of antigen repair buffer for 10 min, followed by incubation at room temperature for 20 min with an antibody cocktail including Alexa Fluor (AF) 488-conjugated anti-Ki67, AF 594-conjugated anti-p16, and Cy5-conjugated anti-CD31. The tissue fixative (Cytelligen) was dropped on the slides, which were subsequently dried overnight. Then, FISH was performed with the centromere probe 8 (CEP 8) SpectrumOrange (Vysis, Abbott Laboratories, Chicago, IL, USA) as described previously [20]. Briefly, the slides were sequentially treated with FR1, FR2, and FR3 and dehydrated in absolute ethyl alcohol. Finally, the cells were hybridized with CEP8, washed with FR3 solution, and mounted with iFISH Full Spectrum Anti-Fade Mounting Medium (Cytelligen).

The protocol of co-immunofluorescence staining of Ki67 and p16 in HeLa cells either growing on the coverslip or being stored in the cell preservation reagent was same to that described above. Fluorescence conjugation of all antibodies was performed in house at Cytelligen.

Automated image scanning and analyses

Images of aneuploid TCs and TECs on coated and formatted CTC slides (Cytelligen) were captured and analyzed via an automatic Metafer-iFISH 3D scanning and image analysis system. Five-channel automated X-Y scanning with cross-Z-sectioning of all the cells was performed at depths of 1 mm (DAPI, CD31, CEP8, p16, and Ki67). Automatic image processing, classification, and statistical analysis were performed on the basis of the expression of tumor markers and chromosome ploidy.

Statistical analysis

All the data were statistically analyzed via IBM SPSS software (version 26.0) and GraphPad Prism software (version 8.0). Differences in continuous variables between groups were compared via the Kruskal–Wallis H test, and all data were presented as the median with interquartile

range. Nonparametric receiver operating characteristic (ROC) curve analysis was used to compare low-grade (≤LSIL) and high-grade (≥HSIL) cervical lesions. A threshold was subsequently established for the number of aneuploid TCs and TECs, and the maximum Youden index (sensitivity + specificity − 1) was used to determine the cutoff value. All data in this study were expressed as a ratio of 10,000%, and logarithms with base 10(lg function) were displayed in the graph. $p < 0.05$ was considered statistically significant.

Results

Identification of aneuploid TCs and TECs

To examine expression and distribution pattern of Ki67 and p16, cervical cancer cell line cells HeLa and pap smear specimens were co-immunostained with mAbs anti-Ki67 and p16. Heterogeneous localization of Ki67 was observed in HeLa cells and clinical samples, showing nucleolus, nucleus and cytoplasm staining, respectively. p16 was observed in either nucleus or cytoplasm of both HeLa cells and clinical specimens.

Images of iFISH identified cells in clinical specimens captured utilizing an automated image scanning and analyzing system are shown in Fig. 1. In accordance with previous studies [21, 22], we defined aneuploid TCs as those with $DAPI^+/CD31^-/CEP8 > 2$ and aneuploid TECs as those with $DAPI^+/CD31^+/CEP8 > 2$. Then, aneuploid TC and TEC subtypes, including triploid, tetraploid, and multiploid (≥pentaploid) TCs and TECs were counted. On the other hand, haploids were not counted due to the small sample size, and no significant difference was detected in the preliminary experiment. p16 and Ki67 have been identified as tumor markers for high-grade cervical lesions in clinical practice [23]. The expression of p16 and Ki67 on TCs and TECs was observed in the present study.

Distribution of aneuploid TCs and TECs in different cervical lesion stages

The results of the comparisons of the distributions of aneuploid TCs and TECs in different stages of cervical lesions are presented in Fig. 2 as lg values [(total number of aneuploid cells/slide cells) × 10,000 + 1]. Interestingly, different proportions of aneuploid TCs were detected in normal cervices infected with hrHPVs, and the proportion of aneuploid TCs increased gradually with increasing severity of cervical lesions, however, no significant difference was observed between the normal and LSIL groups, but the differences among the other groups were statistically significant (Fig. 2A), this phenomenon was not obvious in aneuploid TECs (Fig. 2B). Next, we analyzed the proportion of $p16^+$ and/or $Ki67^+$ ($p16/Ki67^+$) aneuploid TCs and TECs. Images revealed that the positive rate of p16/Ki67 increased with the severity of the cervical lesions. Additionally, the proportion of $p16/Ki67^+$ aneuploid TCs in cervical cancer was significantly greater than that in HSIL, LSIL, and normal cervix, but this difference was not significant for aneuploid TECs (Fig. 2C, D).

Subclassification of aneuploid TCs and TECs by chromosomal ploidy

To further understand the distribution and clinical significance of aneuploid TCs and TECs with different chromosome ploidies at all stages of cervical lesions, we divided aneuploid TCs and TECs into 12 subtypes. The results revealed that the difference between the normal and LSIL groups was not statistically significant for any aneuploid subclass of TCs or TECs. Among all subtypes of aneuploid TCs, the proportion of tetraploid and ≥pentaploid TCs in patients with HSIL and cervical cancer was significantly greater than that in patients with mild lesions, although the distributions of the triploid TCs were similar, they could not distinguish between LSIL and HSIL (Fig. 3A). For aneuploid TECs, the alteration trend of the proportion in each subclass was irregular, and only TECs with ≥pentaploid ploidy could distinguish cervical cancer from HSIL, LSIL, and normal cervix (Fig. 3B).

In the analysis of $p16/Ki67^+$ aneuploid TCs and TECs, the positive rate of p16/Ki67 in each subclass of aneuploid TCs increased with the severity of the cervical lesions (Fig. 3C). First, the results of the analysis of triploid TCs revealed that the positive rate of p16/Ki67 in the cancer group was much greater than that in the HSIL, LSIL, and normal groups. Compared with triploid tumor cells, $p16/Ki67^+$ tetraploid

(See figure on next page.)

Fig. 1 Detection of aneuploid TCs and TECs in cervical exfoliated cells of patients with cervical lesions by iFISH. **A** Heterogeneous localization of Ki67 and p16 in cervical cancer HeLa cells. Ki67 is observed in nucleolus of HeLa cells cultured on the coverslip (a) and in nucleus as well as partially in nucleolus of trypsinized HeLa cells stored in the preservation solution (b). p16 localizes in cytoplasm under both conditions. **B** Representative images of aneuploid $CD31^-$ TCs in clinical pap smear specimens examined by iFISH. Aneuploid TCs are defined as $DAPI^+/CD31^-/CEP8 > 2$ with or without Ki67 and/or p16 expression. **C** Representative images of aneuploid $CD31^+$ TECs in pap smear specimens. TECs are defined as $DAPI^+/CD31^+/CEP8 > 2$ with or without Ki67 and/or p16 expression. Bar, 5 μm. Similar to HeLa cells (A), heterogeneous localization of Ki67 and p16 is found in TCs (B) and TECs (C), which is same to that previously reported by others

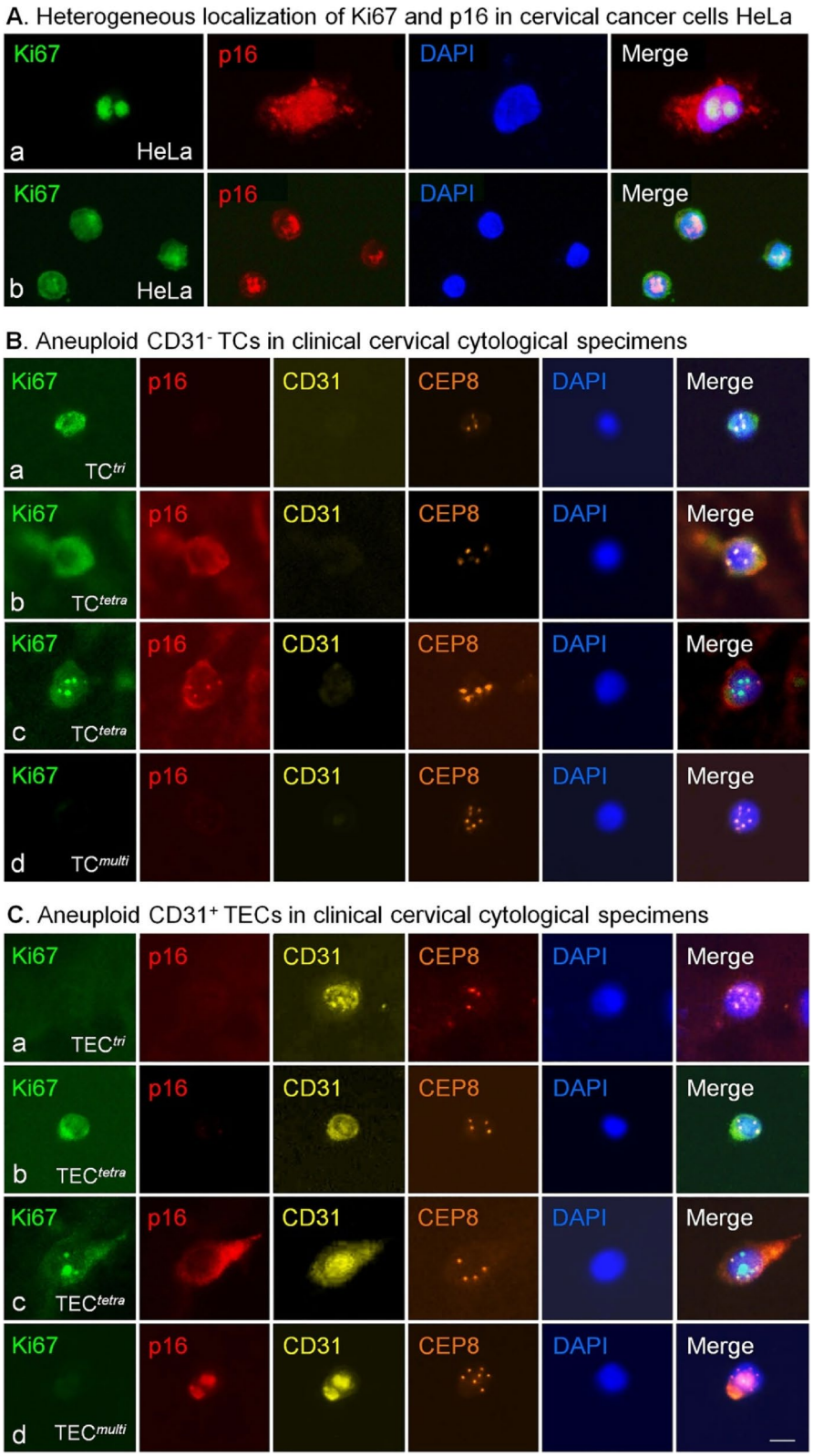

Fig. 1 (See legend on previous page.)

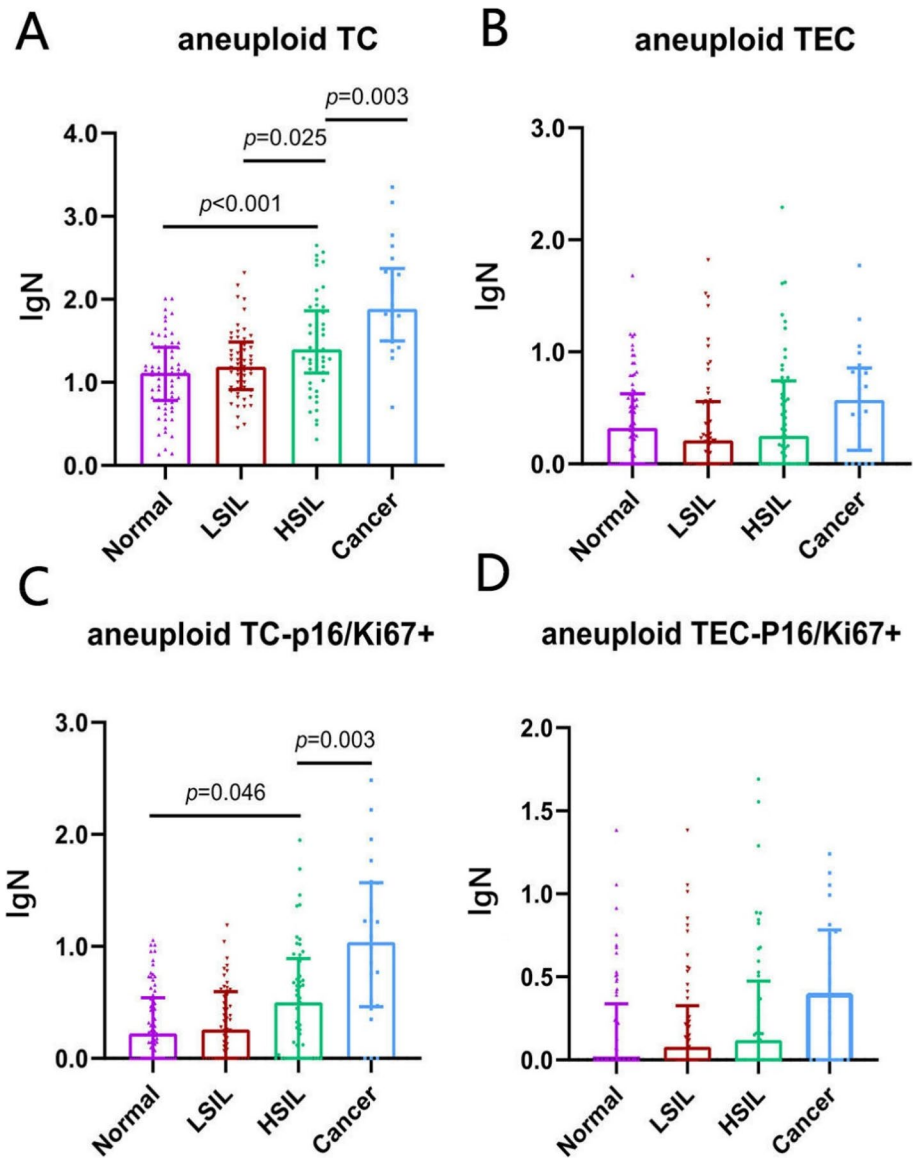

Fig. 2 Distribution of aneuploid TCs and TECs at different stages of cervical lesions. N = total number of abnormal cells/slide cells) × 10,000 + 1. H value: $H_A = 40.469$, $H_B = 4.907$, $H_C = 23.581$, $H_D = 7.563$

TCs were distinguished between patients with HSIL and those with milder lesions. On the other hand, the proportion of ≥ pentaploid TCs that were p16/Ki67$^+$ could distinguish all stages of cervical lesions well except between the normal and LSIL groups, and the significance was better than that in p16/Ki67$^+$ triploid and tetraploid TCs. The current data indicate that the higher the ploidy is, the greater the degree of chromosomal instability is, thus making the cells conducive to the development of malignant tumors. Therefore, the positive rates of tumor markers in aneuploid TCs at different grades of cervical lesions differ markedly. However, this phenomenon did not occur in all subclasses of TECs. As shown in Fig. 3D, no significant difference was detected in the positive rate of target cells among all groups except for the difference in ≥ pentaploid TECs between cancer and LSIL groups. This suggests that the multiploidy TECs will only show a significant increase during the cancer stage.

Distribution of aneuploid TCs and TECs in precancerous lesions caused by HPV16/18 infections versus non-HPV16/18 infections

The management strategies for individuals with a normal cervix and LSIL differ between those with

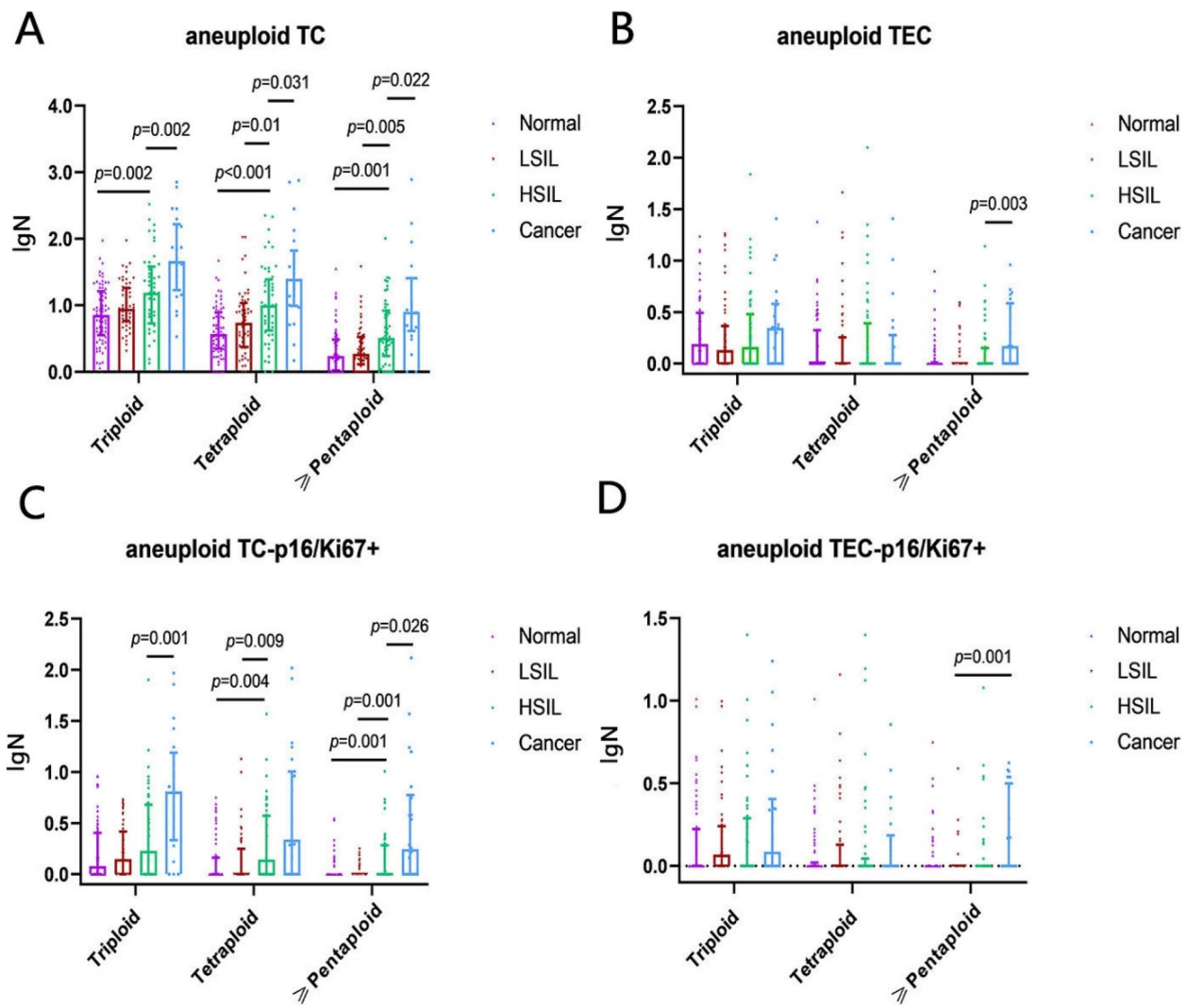

Fig. 3 Distribution of aneuploid TC and TEC subtypes at different stages of cervical lesions. *H* value: **A** $H_{A\,tri}=32.960$, $H_{A\,tetra}=37.982$, $H_{A\,multi}=33.139$. **B** $H_{B\,tri}=1.384$, $H_{B\,tetra}=0.660$, $H_{B\,multi}=16.390$. **C** $H_{C\,tri}=23.737$, $H_{C\,tetra}=21.888$, $H_{C\,multi}=32.664$, (**D**) $H_{D\,tri}=3.988$, $H_{D\,tetra}=0.859$, $H_{D\,multi}=12.249$

HPV16/18 infections and those with non-HPV16/18 infections. Furthermore, there is variation in the clearance of HPV and the recurrence rates of lesions after HSIL treatment. Therefore, clarifying the distribution of aneuploid TCs and TECs in different HPV types might aid in the tailored management of precancerous lesions. Following stratification on the basis of HPV type, our findings revealed that the distribution of aneuploid TCs and TECs differed from the overall trend. Specifically, for patients with HPV16/18 infection, the number of aneuploid TCs in the LSIL group was significantly greater than that in the normal group, whereas no significant difference was detected between the LSIL and HSIL groups (Fig. 4A). In contrast, for patients with non-HPV16/18 infections, the distribution of aneuploid TCs was obviously different between the LSIL and HSIL groups (Fig. 4C), suggesting that the progression of lesions may vary in speed between HPV16/18 and non-HPV16/18 infections, with HPV16/18-infected patients potentially experiencing rapid lesion progression at an earlier stage. The corresponding p16/Ki67 positivity rates in the HPV16/18-positive group tended to increase overall, although the difference was not significant (Fig. 4B). In contrast, no discernible difference was evident in the non-HPV16/18-positive group (Fig. 4D). Similarly, these differences were not reflected in the distribution of aneuploid TECs (Fig. 5).

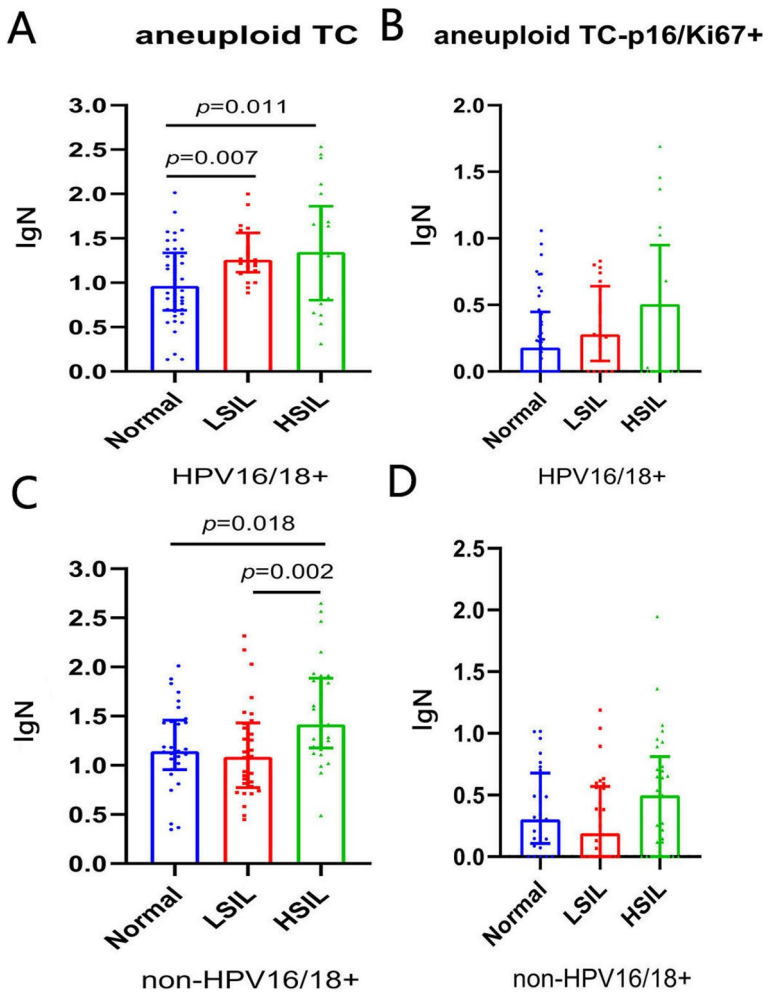

Fig. 4 Distribution of aneuploid TCs at different stages of cervical lesions after discriminating HPV types. *H* value: $H_A = 10.245$, $H_B = 5.077$, $H_C = 10.629$, $H_D = 2.717$

Subclassification of chromosomal ploidy of aneuploid TCs and TECs in precancerous lesions caused by HPV16/18 infections versus non-HPV16/18 infections

In the HPV16/18 group, significant differences were observed in all subtypes of aneuploid TCs between the normal cervix and both the LSIL and the HSIL. Notably, the differences were most pronounced in triploid and tetraploid TCs (Fig. 6A). In contrast, for non-HPV16/18 infections, only tetraploid and ≥ pentaploid TCs exhibited significant differences between the HSIL and both the LSIL and the normal cervix (Fig. 6C). For p16/Ki67$^+$ aneuploid TCs in HPV16/18 infections, tetraploid and ≥ pentaploid TCs presented differences between the normal cervix and HSIL, in addition, tetraploid TCs could distinguish LSIL from HSIL (Fig. 6B). In non-HPV16/18 infections, only ≥ pentaploid TCs could effectively distinguish LSIL from HSIL (Fig. 6D). Nevertheless, across all subtypes of TECs, no apparent difference emerged in the number of triploid, tetraploid, or ≥ pentaploid TECs among the different groups (Fig. 7).

Identification of HSIL$^+$ by individual and combined aneuploid TC and TEC counts

Given that the clinical treatment focuses on HSIL and above lesions (HSIL$^+$), we divided the pathology results into two groups: patients with ≤ LSIL and patients with ≥ HSIL. The ROC curve was plotted to evaluate the diagnostic value of each subcategory in the prediction of HSIL$^+$ (Fig. 8). Next, we selected the best cutoff values on the basis of the maximum value of the Youden index, and the corresponding sensitivity and specificity are shown in Table 2. The area under the curve (AUC) of tetraploid TCs was the largest (AUC = 0.739, cutoff value: 8.83, sensitivity: 60.3%, specificity: 80.5%), followed by ≥ pentaploid TCs (AUC = 0.724, cutoff value: 1.74, sensitivity: 69.9%, specificity: 69.9%) and

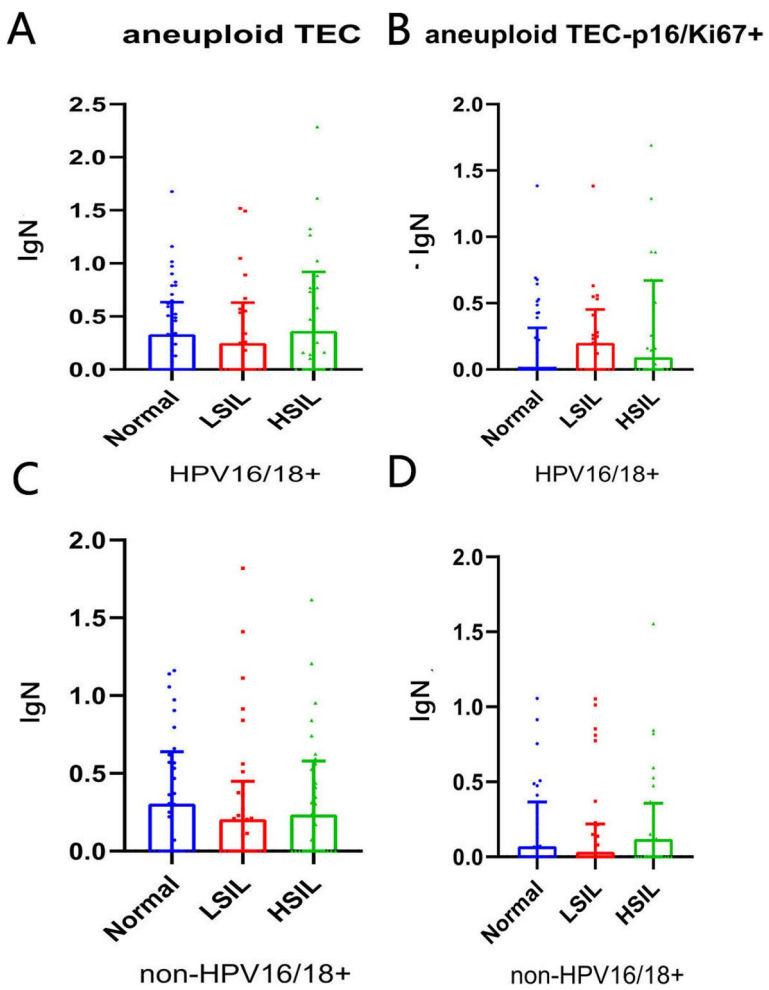

Fig. 5 Distribution of aneuploid TECs at different stages of cervical lesions after discriminating HPV types (A, C). *H* value: $H_A = 1.179$, $H_B = 2.426$, $H_C = 0.809$, $H_D = 0.354$

triploid TCs (AUC = 0.699, cutoff value: 24.73, sensitivity: 45.2%, specificity: 89.4%). However, the analytical results obtained from aneuploid TCs and TECs positive for p16/Ki67 were unsatisfactory. The AUC values were small, and the sensitivity of aneuploid TCs with positive p16/Ki67 was much lower than expected, while the specificity was satisfactory. In addition, among these aneuploid TCs, the specificity of ≥ pentaploid TCs with positive p16/Ki67 expression was the highest (88.6%), followed by tetraploid TCs with positive p16/Ki67 expression (78.9%) and triploid TCs with positive p16/Ki67 expression (64.4%). Together, the diagnostic value of a single subclass is reflected mainly in its specificity. Next, we combined some subclasses, and the AUC value of ≥ tetraploid TCs was the largest (AUC = 0.745, cutoff value: 8.74, sensitivity: 71.2%, specificity: 74.8%). The sensitivity and specificity of the other combinations are shown in Table 2.

Discussion

In this study, we evaluated the variation in the number of chromosome 8 aneuploid TCs and TECs at different stages of the cervical lesion and different HPV types. Additionally, the diagnostic value of aneuploidy subtypes and their combinations for $HSIL^+$ patients was determined. The results revealed that the distribution of aneuploid TCs varied with the severity of the cervical lesions, indicating that they are optimal indicators of the CIN stage but cannot be found in aneuploid TECs. The subtype analysis of aneuploidy revealed that triploid, tetraploid, and ≥ pentaploid TCs could distinguish between HSIL, cervical cancer, and milder lesions and had good clinical value in the diagnosis of $HSIL^+$, especially in terms of specificity. Compared with subtypes, ≥ pentaploid TCs had preferable sensitivity (69.9%), whereas triploid TCs had preferable specificity

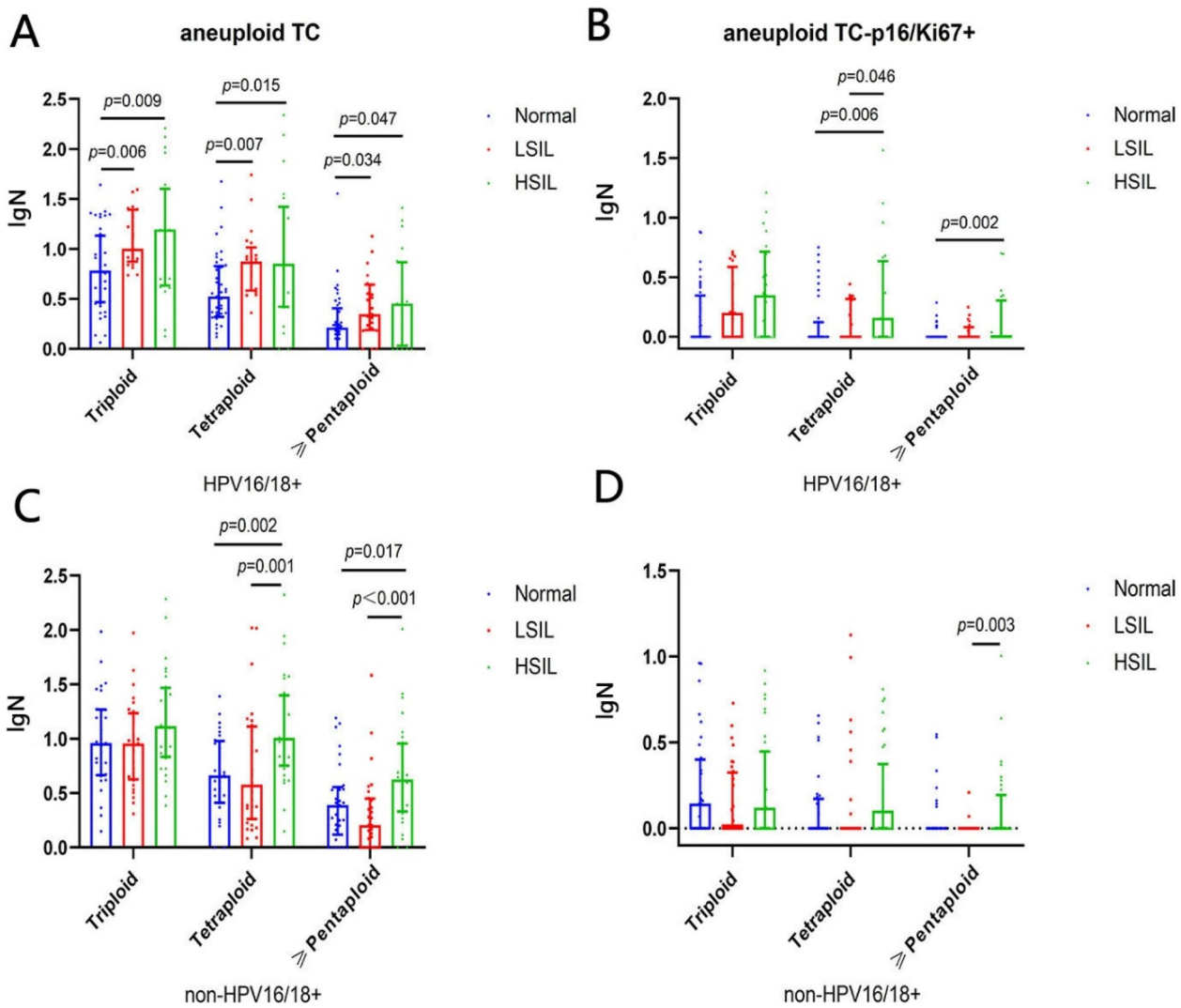

Fig. 6 Distribution of aneuploid TC subtypes at different stages of cervical lesions after discriminating HPV types. *H* value: **A** $H_{A\,tri}=10.492$, $H_{A\,tetra}=9.787$, $H_{A\,multi}=6.256$. **B** $H_{B\,tri}=4.538$, $H_{B\,tetra}=7.722$, $H_{B\,multi}=9.629$. **C** $H_{C\,tri}=4.552$, $H_{C\,tetra}=13.499$, $H_{C\,multi}=14.036$. **D** $H_{D\,tri}=0.855$, $H_{D\,tetra}=4.331$, $H_{D\,multi}=8.682$

(89.4%). However, the sensitivity and specificity of some subcategory combinations did not improve.

Previous analyses of cervical cytology focused on DNA content measurement, and the aneuploidy of DNA aided in the diagnosis of cervical lesions [24, 25]. However, in some cells, although the average amount of DNA is close to that of diploids, the true diploid regions may be missing [26]. Conversely, aneuploidy karyotype detection is objective. In normal human cells, aneuploidy is rare and most autosomal aneuploidy cells are embryonically lethal [8]. Strikingly, only tumor cells can maintain or increase their proliferation rate when they exhibit aneuploidy. Carcinogenic HPV plays a critical role in inducing cervical cellular aneuploidy, and HPV oncoproteins (especially E6 and E7) lead to mitotic defects through mediating cell cycle regulation disorders and affecting centrosome replication and spindle polarity, thus inducing aneuploidy [11]. Previous studies have shown that the production of tetraploids occurs during early-stage events of cervical cancer, which predisposes cervical cells to aneuploidy [10, 11]. Our findings are similar when aneuploidy progresses to tetraploidy, the difference in the number of aneuploid TCs between LSIL and HSIL begins to make sense (Fig. 3A). Women with higher levels of tetraploid TCs in exfoliated cervical cells should be our priority for follow-up. Moreover, ≥ pentaploidy seems more obvious in cervical cancer, suggesting that a higher ploidy level is more relevant to the severity of malignancy. Aneuploidy

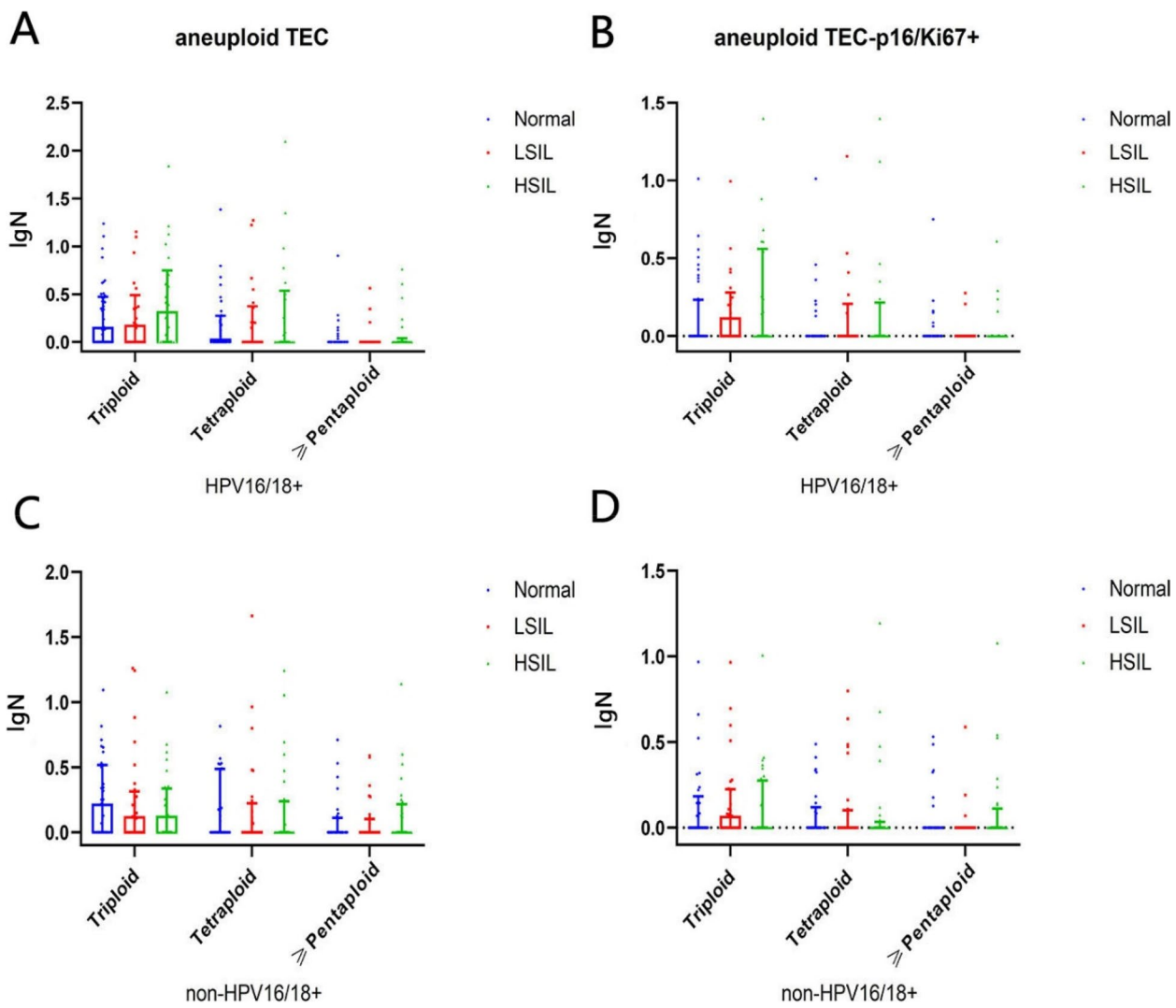

Fig. 7 Distribution of aneuploid TEC subtypes at different stages of cervical lesions after discriminating HPV types. *H value:* **A** $H_{A\,tri}=1.037$, $H_{A\,tetra}=0.054$, $H_{A\,multi}=0.831$. **B** $H_{B\,tri}=2.555$, $H_{B\,tetra}=1.855$, $H_{B\,multi}=0.925$. **C** $H_{C\,tri}=0.782$, $H_{C\,tetra}=1.172$, $H_{C\,multi}=0.658$. **D** $H_{D\,tri}=0.265$, $H_{D\,tetra}=0.233$, $H_{D\,multi}=2.961$

is a form of chromosomal instability, and detecting karyotypic alterations provides abundant genetic information on tumor progression, which may help us recognize the increased invasiveness and aggressiveness of cervical cancer. Multiple genome sequencing analyses revealed that most of the chromosome arms of cervical cancer cells were gained or lost in different proportions [14, 27], and additional studies should track karyotype changes during tumor progression and after treatment because the aneuploid karyotype is associated with tumor evolution and drug resistance [28].

HPV16 and 18 pose a several-fold greater risk of developing high-grade cervical lesions than other high-risk HPV infections [29]. Consequently, follow-up and treatment strategies for HPV16/18-infected patients are more aggressive. Our data indicated that the stages of aneuploid TC proliferation differ between HPV16/18-infected and non-HPV16/18-infected patients. Specifically, aneuploid TCs increased mainly during LSIL in HPV16/18-infected patients but more prominently in HSIL for non-HPV16/18 cases. These findings suggest that HPV16/18 infections can progress rapidly over a short period, even in LSIL, cells exhibit high aneuploidy, potentially progressing to HSIL as it often signals malignant potential. However, this conclusion requires confirmation through long-term follow-up studies with larger sample sizes. Therefore,

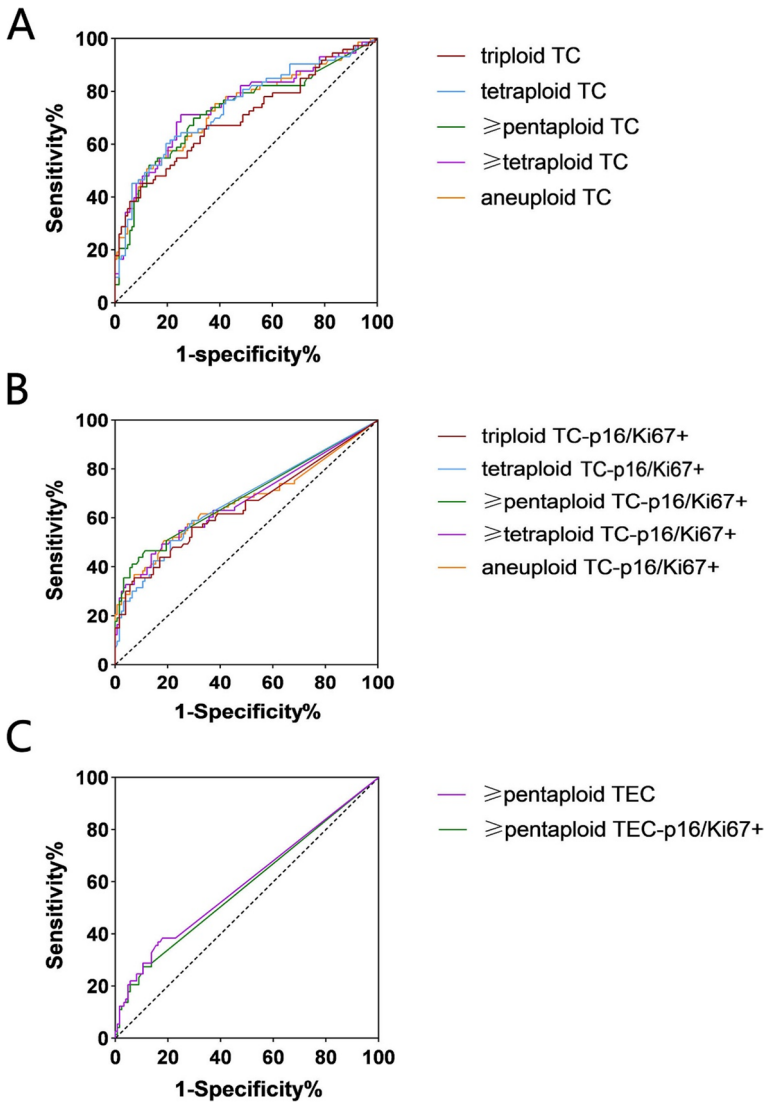

Fig. 8 Receiver operating characteristic (ROC) analysis of aneuploid TCs and TECs

Table 2 Optimum cut-off values and their respective sensitivity and specificity

Index	cut-off(per 10,000)	AUC	Sensitivity	Specificity	*P*	95%CI
triploid TC	24.73	0.699	45.20%	89.40%	< 0.001	0.619–0.778
tetraploid TC	8.83	0.739	60.30%	80.50%	< 0.001	0.663–0.814
≥ pentaploid TC	1.74	0.724	69.90%	69.90%	< 0.001	0.646–0.802
≥ tetraploid TC	8.74	0.745	71.20%	74.80%	< 0.001	0.670–0.820
aneuploid TC	38.71	0.734	50.70%	87.80%	< 0.001	0.658–0.810
triploid TC-p16/Ki67 +	3.65	0.646	35.60%	64.40%	0.001	0.562–0.730
tetraploid TC-p16/Ki67 +	0.66	0.670	50.70%	78.90%	< 0.001	0.589–0.751
≥ pentaploid TC-p16/Ki67 +	0.36	0.684	46.60%	88.60%	< 0.001	0.602–0.767
≥ tetraploid TC-p16/Ki67 +	1.28	0.668	49.30%	82.10%	< 0.001	0.585–0.752
aneuploid TC-p16/Ki67 +	3.33	0.663	50.70%	81.30%	< 0.001	0.578–0.747
≥ pentaploid TEC	0.35	0.595	37.00%	83.70%	0.026	0.510–0.680
≥ pentaploid TEC-p16/Ki67 +	0.35	0.580	27.40%	89.40%	0.06	0.495–0.665

aggressive treatment may be more reasonable than conservative follow-up for LSIL patients with HPV16/18 infection.

Furthermore, upon subclassification of aneuploid TCs, we found significant differences in the distribution of ≥ pentaploid TCs in HSIL were more remarkably present in the non-HPV16/18 infection group. This may suggest an intensification of chromosomal instability and a worse prognosis with greater malignancy potential during future disease progression. Multiple previous studies have reported that patients with HPV16/18-infected cervical cancer have a better prognosis than non-HPV16/18-infected patients, with higher overall survival (OS) and progression-free survival (PFS) rates, which may be related to the higher sensitivity of HPV16/18-infected cervical cancer to radiotherapy and chemotherapy [30, 31]. Chromosomal instability can lead to the acquisition of chemotherapy resistance in tumors. Compared with diploid tumors, tetraploid TCs exhibit greater tumorigenicity and are prone to developing resistance to conventional chemotherapeutic drugs [32, 33]. This, to some extent, explains why HPV16/18-infected cervical cancer are more sensitive to radiotherapy and chemotherapy, and we can observe that the growth of tetraploid TCs in HSIL was more obvious in the non-HPV16/18-positive group, as shown in Fig. 6C. Subclassified aneuploid TCs may also serve as independent predictors of chemotherapy response and prognosis in cervical cancer patients.

Chromosome 8 abnormalities are closely related to the occurrence and development of various tumors, many cancer-related genes are located on this chromosome, especially *c-MYC* [34, 35]. The amplification of CEP8 has been widely used to evaluate hematological tumors and various solid tumors [36, 37]. Abnormalities in chromosome 8, especially the trisomy of chromosome 8, have also been confirmed to exist in cervical cancer patients in previous studies [38]. iFISH was mainly introduced for detecting circulating TCs and TECs by utilizing CEP8 probe. Many clinical studies have shown that iFISH has great clinical significance in the early diagnosis of tumors, the evaluation of curative effects and prognosis, and the resistance and recurrence of tumors [21, 22, 39, 40]. For example, Cheng H et al. reported that the combined detection of triploid and tetraploid circulating TCs or triploid and tetraploid small-cell circulating TCs has high sensitivity and specificity in distinguishing ovarian cancer patients from those with benign tumors [21]. To the best of our knowledge, this is the first study in which the above technique was applied for the detection of aneuploidy in exfoliated cervical cells, confirming the difference in the distribution of chromosome 8 aneuploidy and its subclasses in cervical lesions at all stages. Previous research on chromosomal changes focused on some chromosomal regions, and their sensitivity values for the detection of $HSIL^+$ were better. In contrast, our specificity is superior to that of their probe sites (such as 3q26&53.3%, 5p15&56.7%, and 20q13&56.7%) [13, 41], possibly because of the change in the copy number of chromosome arms and bands precedes genome-wide polyploidy.

p16 and Ki67 are the most frequently used diagnostic tumor markers for identifying $HSIL^+$. Several studies have shown that the sensitivity of p16/Ki67 double-staining for the diagnosis of $HSIL^+$ is significantly greater than that of cervical cytology, although the improvement in specificity is not significant [42, 43]. Interestingly, our results indicated that p16/Ki67 double-staining had a preferable specificity for diagnosing $HSIL^+$, however, the sensitivity was not satisfactory. The differences in these results may be attributed to two factors. First, false positives may occur because p16 is expressed in endometrial tubal metaplasia and cervical endometriosis [43]. Second, our study only estimated the expression of p16/Ki67 on chromosome 8 in aneuploid tumor cells, but omitted $p16/Ki67^+$ diploid tumor cells, which were different from the number of tumor marker-positive cells reported in other studies. Our study also observed some $p16/Ki67^+$ diploid cells, therefore, we cannot rely solely on markers to identify tumor cells via nonmorphological detection because of the uncertainty of whether these cells are normal or have abnormal chromosome structures. Thus, additional aneuploidy testing may accurately identify tumor cells. Strikingly, E6/E7 play a leading role in the formation of aneuploid cervical cells, perhaps they are more appropriate as phenotypes to be combined with karyotypic detection.

Another focus of our study was aneuploid TECs. Unlike normal blood vessels, tumor blood vessels mainly consist of abnormal endothelial cells with aneuploid chromosomes, which exhibit traits of tumor cells and promote tumorigenesis, progression, and metastasis [44, 45]. CD31 is the marker of endothelial cells. Our data revealed that the number of $CD31^+$ aneuploid TECs altered dynamically at different stages of cervical lesions and significantly increased in cancerous cells, especially those with ≥ pentaploid TECs, suggesting that aneuploid TECs support tumor progression. Moreover, the positive rate of p16/Ki67 aneuploid TECs increased with the severity of cervical lesions, although no significant difference was noted in each subclassification. Interestingly, these dynamic changes were similar to those reported previously [22]. The diagnostic role of aneuploid TECs is not remarkable, whereas the presence of aneuploid TECs is crucial for antiangiogenic therapy, as chromosomal instability may provide a mechanism to alter endothelial cells and render them resistant to drugs [46, 47]. Some

researchers have proposed that aneuploid TECs are more resistant to chemotherapeutic drugs like vincristine and 5-fluorouracil than normal endothelial cells [48]. Therefore, their potential therapeutic value seems promising for in-depth investigation.

Limitations

Nevertheless, the present study has several shortcomings. First, the quantity of cells in different samples varies greatly due to the individualized clinical practice of sample collection for each patient. Second, although the number of aneuploid tumor cells in peripheral blood is extremely low in normal subjects, as previously reported by others, the existence of aneuploid cells in the cervix of a large cohort of non-HPV-infected healthy subjects remains to be examined. In addition, whether specific subpopulations of aneuploid TCs and TECs and their dynamic changes can predict HPV clearance is still uncertain. Thus, additional large cohort clinical studies should be conducted to further optimize and validate aneuploidy and tumor marker-derived biomarkers for maximal benefit in the clinical diagnosis of cervical lesions.

Conclusions

In this study, iFISH, a novel detection technology, was used to detect, characterize, and classify aneuploid TCs and TECs in exfoliated cells of cervical lesions. The current findings indicate that aneuploid TCs and TECs exhibit differences in the quantity, degree, and expression of tumor markers across all stages of cervical lesions. Aneuploid gains were correlated with the severity of cervical lesions. Furthermore, the growth of aneuploid TCs induced by HPV16/18 infection mainly emerges at the early stage compared with that of other HPV types. Triploid, tetraploid, and ≥ pentaploid TCs, regardless of p16/Ki67 expression, can distinguish $HSIL^+$ with high specificity.

Abbreviations

HPV	Human papillomavirus
TC	Tumor cell
TEC	Tumor endothelial cell
LSIL	Low-grade squamous intraepithelial lesion
HSIL	High-grade squamous intraepithelial lesion
FISH	Fluorescence in situ hybridization
CEP8	Centromere probe 8

Acknowledgements

The authors thank staff at Shanghai General Hospital, Cytointelligen (China Medical City, Taizhou, Jiangsu, China) and Cytelligen (San Diego, CA, USA) for providing support.

Authors' contributions

Y.L.W. contributed conceptualization, validation, formal analysis, investigation, resources, and writing original draft; A.Y.L. and D.D.W. contributed methodology and validation; P.P.L. contributed conceptualization, visualization, writing – original draft, review and editing; X.X.Z contributed data curation, methodology and writing original draft; Y.B.Y contributed review, editing and funding acquisition; Y.P.Z contributed project administration, conceptualization, resources and supervision. All the authors read and approved the final version of manuscript.

Funding

This research was funded by the Shanghai Pujiang Talent Plan (18PJC097) to Y.B.Y., the Shanghai Aging and Women and Children's Health Research Project (2020YJZX0215) to Y.B.Y.

Data availability

No datasets were generated or analysed during the current study.

Declarations

Ethics approval and consent to participate

All procedures were performed according to the Declaration of Helsinki. The study was approved by the Ethics Committee of the Shanghai General Hospital (reference 2021SQ263). All patients provided informed consent prior to cervical cytological specimen collection.

Consent for publication

Not applicable.

Competing interests

The authors declare no competing interests.

Author details

[1]Department of Gynecology and Obstetrics, Shanghai General Hospital, Shanghai Jiao Tong University School of Medicine, Shanghai, China. [2]Cytelligen, San Diego, CA, USA.

Received: 25 April 2024 Accepted: 16 May 2025
Published online: 26 May 2025

References

1. Sung H, Ferlay J, Siegel RL, Laversanne M, Soerjomataram I, Jemal A, Bray F. Global Cancer Statistics 2020: GLOBOCAN Estimates of Incidence and Mortality Worldwide for 36 Cancers in 185 Countries. CA Cancer J Clin. 2021;71(3):209–49.
2. Moscicki AB, Schiffman M, Burchell A, Albero G, Giuliano AR, Goodman MT, Kjaer SK, Palefsky J. Updating the natural history of human papillomavirus and anogenital cancers. Vaccine. 2012;30(Suppl 5):F24-33.
3. Xia C, Hu S, Xu X, Zhao X, Qiao Y, Broutet N, Canfell K, Hutubessy R, Zhao F. Projections up to 2100 and a budget optimisation strategy towards cervical cancer elimination in China: a modelling study. The Lancet Public Health. 2019;4(9):e462–72.
4. Wright TC, Stoler MH, Behrens CM, Sharma A, Sharma K, Apple R. Interlaboratory variation in the performance of liquid-based cytology: Insights from the ATHENA trial. Int J Cancer. 2014;134(8):1835–43.
5. Orumaa M, Innos K, Suurna M, Salumäe L, Veerus P: Quality Assessment of Cervical Cytology Practices in Estonia From. to 2018. Cancer Control. 2007;2022:29.>
6. Tang HP, Cai D, Kong YQ, Ye H, Ma ZX, Lv HS, Tuo LR, Pan QJ, Liu ZH, Han X. Cervical cytology screening facilitated by an artificial intelligence microscope: A preliminary study. Cancer Cytopathol. 2021;129(9):693–700.
7. Vasudevan A, Schukken KM, Sausville EL, Girish V, Adebambo OA, Sheltzer JM. Aneuploidy as a promoter and suppressor of malignant growth. Nat Rev Cancer. 2021;21(2):89–103.
8. Tanaka K, Hirota T. Chromosomal instability A common feature and a therapeutic target of cancer. Biochim Biophys Acta. 1866;1:64–75.
9. Ben-David U, Amon A. Context is everything: aneuploidy in cancer. Nat Rev Genet. 2020;21(1):44–62.
10. Olaharski AJ, Sotelo R, Solorza-Luna G, Gonsebatt ME, Guzman P, Mohar A, Eastmond DA. Tetraploidy and chromosomal instability are early events during cervical carcinogenesis. Carcinogenesis. 2006;27(2):337–43.

11. Mallick S, Choi Y, Taylor AM, Cosper PF. Human Papillomavirus-Induced Chromosomal Instability and Aneuploidy in Squamous Cell Cancers. Viruses. 2024;16(4):501.
12. Lin PP, Gires O, Wang DD, Li L, Wang H. Comprehensive in situ co-detection of aneuploid circulating endothelial and tumor cells. Sci Rep. 2017;7(1):9789.
13. Luhn P, Houldsworth J, Cahill L, Schiffman M, Castle PE, Zuna RE, Dunn ST, Gold MA, Walker J, Wentzensen N. Chromosomal gains measured in cytology samples from women with abnormal cervical cancer screening results. Gynecol Oncol. 2013;130(3):595–600.
14. Ren T, Suo J, Liu S, Wang S, Shu S, Xiang Y, Lang J-H. Using low-coverage whole genome sequencing technique to analyze the chromosomal copy number alterations in the exfoliative cells of cervical cancer. J Gynecol Oncol. 2018;29(5):e78.
15. Thomas LK, Bermejo JL, Vinokurova S, Jensen K, Bierkens M, Steenbergen R, Bergmann M, von Knebel DM, Reuschenbach M. Chromosomal gains and losses in human papillomavirus-associated neoplasia of the lower genital tract – A systematic review and meta-analysis. Eur J Cancer. 2014;50(1):85–98.
16. Fu Z, Zhang L, Chen R, Zhan J, Zhong J, Zheng W, Zou J, Wang P, Deng X, Lin AY, et al. Biphasic co-detection of melanoma aneuploid tumor cells and tumor endothelial cells in guidance of specifying the field cancerized surgical excision margin and administering immunotherapy. Cancer Lett. 2024;598:217099.
17. Hida K, Klagsbrun M. A New Perspective on Tumor Endothelial Cells: Unexpected Chromosome and Centrosome Abnormalities. Can Res. 2005;65(7):2507–10.
18. Hida K, Maishi N, Annan D, Hida Y. Contribution of Tumor Endothelial Cells in Cancer Progression. Int J Mol Sci. 2018;19(5):1272.
19. Perkins RB, Guido RS, Castle PE, Chelmow D, Einstein MH, Garcia F, Huh WK, Kim JJ, Moscicki AB, Nayar R, et al. 2019 ASCCP Risk-Based Management Consensus Guidelines for Abnormal Cervical Cancer Screening Tests and Cancer Precursors. J Low Genit Tract Dis. 2020;24(2):102–31.
20. Zhang T, Zhang L, Gao Y, Wang Y, Liu Y, Zhang H, Wang Q, Fanbin Hu, Li J, Tan J, et al. Role of aneuploid circulating tumor cells and CD31+ circulating tumor endothelial cells in predicting and monitoring anti-angiogenic therapy efficacy in advanced NSCLC. Mol Oncol. 2021;15(11):2891–909.
21. Cheng H, Wang S, Luan W, Ye X, Dou S, Tang Z, Zhu H, Ping Lin P, Li Y, Cui H, et al. Combined detection and subclass characteristics analysis of CTCs and CTECs by SE-iFISH in ovarian cancer. Chin J Cancer Res. 2021;33(2):256–70.
22. Lei Y, Sun N, Zhang G, Liu C, Lu Z, Huang J, Zhang C, Zang R, Che Y, Mao S, et al. Combined detection of aneuploid circulating tumor-derived endothelial cells and circulating tumor cells may improve diagnosis of early stage non-small-cell lung cancer. Clin Transl Med. 2020;10(3): e128.
23. Perkins RB, Wentzensen N, Guido RS, Schiffman M. Cervical Cancer Screening: A Review. JAMA. 2023;330(6):547–58.
24. Costa AF, Ribeiro MGM, Onofre ASC, Miranda Onofre FB. Aneuploidy detection for diagnostic and prognostic use in premalignant and malignant lesions of the uterine cervix: A systematic review. Diagn Cytopathol. 2020;49(2):335–46.
25. Costa AF, Pogere A, Pasinato APBF, Onofre ASC. Onofre FBdM: DNA image cytometry parameters to identify high-grade cervical lesions. Cytopathology. 2022;33(5):563–71.
26. Lauren M. F. Merlo, Li-san Wang, John W. Pepper, Rabinovitch PS, Maley CC. Polyploidy, aneuploidy and the evolution of cancer. Adv Exp Med Biol. 2010;676:1–13.
27. Bodelon C, Vinokurova S, Sampson JN, den Boon JA, Walker JL, Horswill MA, Korthauer K, Schiffman M, Sherman ME, Zuna RE, et al. Chromosomal copy number alterations and HPV integration in cervical precancer and invasive cancer. Carcinogenesis. 2016;37(2):188–96.
28. Ippolito MR, Martis V, Martin S, Tijhuis AE, Hong C, Wardenaar R, Dumont M, Zerbib J, Spierings DCJ, Fachinetti D, et al. Gene copy-number changes and chromosomal instability induced by aneuploidy confer resistance to chemotherapy. Dev Cell. 2021;56(17):2440-2454.e2446.
29. Hanley SJB, Fujita H, Aoyama-Kikawa S, Kasamo M, Torigoe T, Matsuno Y, Noriaki S. Evaluation of partial genotyping with HPV16/18 for triage of HPV positive, cytology negative women in the COMPACT study. J Gynecol Oncol. 2021;32(6):e86.
30. Onuki M, Matsumoto K, Tenjimbayashi Y, Tasaka N, Akiyama A, Sakurai M, Minaguchi T, Oki A, Satoh T, Yoshikawa H. Human papillomavirus genotype and prognosis of cervical cancer: Favorable survival of patients with HPV16-positive tumors. Papillomavirus Research. 2018;6:41–5.
31. Kuno I, Takayanagi D, Asami Y, Murakami N, Matsuda M, Shimada Y, Hirose S, Kato MK, Komatsu M, Hamamoto R, et al. TP53 mutants and non-HPV16/18 genotypes are poor prognostic factors for concurrent chemoradiotherapy in locally advanced cervical cancer. Sci Rep. 2021;11(1):19261.
32. Coward J, Harding A. Size Does Matter: Why Polyploid Tumor Cells are Critical Drug Targets in the War on Cancer. Front Oncol. 2014;4:123.
33. Galofré C, Gönül Geyik Ö, Asensio E, Wangsa D, Hirsch D, Parra C, Saez J, Mollà M, Yüce Z, Castells A, et al. Tetraploidy-Associated Genetic Heterogeneity Confers Chemo-Radiotherapy Resistance to Colorectal Cancer Cells. Cancers. 2020;12(5):1118.
34. Watkins TBK, Lim EL, Petkovic M, Elizalde S, Birkbak NJ, Wilson GA, Moore DA, Grönroos E, Rowan A, Dewhurst SM, et al. Pervasive chromosomal instability and karyotype order in tumour evolution. Nature. 2020;587(7832):126–32.
35. Qu T, Zhang C, Lu X, Dai J, He X, Li W, Han L, Yin D, Zhang E. 8q24 derived ZNF252P promotes tumorigenesis by driving phase separation to activate c-Myc mediated feedback loop. Nat Commun. 2025;16(1):1986.
36. Ma G, Jiang Y, Liang M, Li J, Wang J, Mao X, Veeramootoo JS, Xia T, Liu X, Wang S. Dynamic monitoring of CD45-/CD31+/DAPI+ circulating endothelial cells aneuploid for chromosome 8 during neoadjuvant chemotherapy in locally advanced breast cancer. Ther Adv Med Oncol. 2020;12:1758835920918470.
37. Dehner C, Moon CI, Zhang X, Zhou Z, Miller C, Xu H, Wan X, Yang K, Mashl J, Gosline SJC, et al. Chromosome 8 gain is associated with high-grade transformation in MPNST. JCI Insight. 2021;6(6):e146351.
38. Mark HF, Feldman D, Samy M, Sun C, Das S, Mark S, Lathrop J. Assessment of Chromosome 8 Copy Number in Cervical Cancer by Fluorescent in situ Hybridization. Exp Mol Pathol. 1999;66(2):157–62.
39. Wang Y, Nong J, Lu B, Gao Y, Hu M, Chen C, Zhang L, Tan J, Yang X, Lin PP, et al. Disseminated tumor cells in bone marrow as predictive classifiers for small cell lung cancer patients. Journal of the National Cancer Center. 2024;4(4):335–45.
40. Li Y, Jiang L, Chen Y, Li Y, Yuan J, Lu J, Zhang Z, Liu S, Feng X, Xiong J, et al. Specific lineage transition of tumor-associated macrophages elicits immune evasion of ascitic tumor cells in gastric cancer with peritoneal metastasis. Gastric Cancer. 2024;27(3):519–38.
41. Polichi FA, Song M, Sitailo S, O'Hare A, Ashfaq R, Muller CY, Morrison LE, King W, Sokolova IA. Analysis of genetic copy number changes in cervical disease progression. BMC Cancer. 2010;10(1):432.
42. Chen X, Chen C, Liu L, Dai W, Zhang J, Han C, Zhou S. Evaluation of p16/Ki-67 dual-stain as triage test for high-risk HPV -positive women: A hospital-based cross-sectional study. Cancer Cytopathol. 2022;130(12):955–63.
43. Dovnik A, Repše Fokter A. The Role of p16/Ki67 Dual Staining in Cervical Cancer Screening. Curr Issues Mol Biol. 2023;45(10):8476–91.
44. Akino T, Hida K, Hida Y, Tsuchiya K, Freedman D, Muraki C, Ohga N, Matsuda K, Akiyama K, Harabayashi T, et al. Cytogenetic Abnormalities of Tumor-Associated Endothelial Cells in Human Malignant Tumors. Am J Pathol. 2009;175(6):2657–67.
45. Lin PP. Aneuploid Circulating Tumor-Derived Endothelial Cell (CTEC): A Novel Versatile Player in Tumor Neovascularization and Cancer Metastasis. Cells. 2020;9(6):1539.
46. Vitale I, Manic G, Senovilla L, Kroemer G, Galluzzi L. Karyotypic Aberrations in Oncogenesis and Cancer Therapy. Trends in Cancer. 2015;1(2):124–35.
47. Morimoto M, Maishi N, Hida K. Acquisition of drug resistance in endothelial cells by tumor-derived extracellular vesicles and cancer progression. Cancer Drug Resist. 2024;7:1.
48. Hida K, Hida Y, Shindoh M. Understanding tumor endothelial cell abnormalities to develop ideal anti-angiogenic therapies. Cancer Sci. 2008;99(3):459–66.

Publisher's Note